Mon. Not. R. Astron. Soc. **000**, 1–4 (2009) Printed 4 March 2009 (MN LATEX style file v2.2)

# The pulsar synchrotron: coherent radio emission

I. Contopoulos⋆
*Research Center for Astronomy, Academy of Athens, 4 Soranou-Efessiou Str., Athens 11527, Greece*



Accepted 2009 March 3. Received 2009 February 10; in original form 2008 November 11

**ABSTRACT**

We propose a simple physical picture for the generation of coherent radio emission in the axisymmetric pulsar magnetosphere that is quite different from the canonical paradigm of radio emission coming from the magnetic polar caps. In this first paper we consider only the axisymmetric case of an aligned rotator. Our picture capitalizes on an important element of the MHD representation of the magnetosphere, namely the separatrix between the corotating closed-line region (the 'dead zone') and the open field lines that originate in the polar caps. Along the separatrix flows the return current that corresponds to the main magnetospheric electric current emanating from the polar caps. Across the separatrix, both the toroidal and poloidal components of the magnetic field change discontinuously. The poloidal component discontinuity requires the presence of a significant annular electric current which has up to now been unaccounted for. We estimate the position and thickness of this annular current at the tip of the closed line region, and show that it consists of electrons (positrons) corotating with Lorentz factors on the order of $10^5$, emitting incoherent synchrotron radiation that peaks in the hard X-rays. These particles stay in the region of highest annular current close to the equator for a path-length of the order of one meter. We propose that, at wavelengths comparable to that path-length, the particles emit coherent radiation, with radiated power proportional to $N^2$, where $N$ is the population of particles in the above path-length. We calculate the total radio power in this wavelength regime and its scaling with pulsar period and stellar magnetic field and show that it is consistent with estimates of radio luminosity based on observations.

**Key words:** pulsars – radio: stars.

## 1 INTRODUCTION

The physical mechanism of pulsar radio emission remains still poorly understood. Observational evidence (e.g. Kramer, Wex & Wielebinski 2000) suggests that it must be due to some coherent radiation mechanism. Unfortunately, neither the exact mechanism (curvature radiation, free electron maser emission, excited plasma waves, etc.), nor its origin (inner or outer magnetosphere) are clear. It is nevertheless widely accepted that radio emission originates within a few stellar radii from the stellar surface, and is due to relativistic plasma outflowing from the two stellar magnetic poles (e.g. Kramer *et al.* 1997).

We here would like to propose a new physical picture for pulsar radio emission that capitalizes on what we have learned about the pulsar magnetosphere when studied under the assumption of force-free ideal magnetohydrodynamics. The first self-consistent solution of the axisymmetric problem (Contopoulos, Kazanas & Fendt 1999, hereafter CKF) demonstrated that the pulsar magnetosphere consists of a closed line corotating region (the so called 'dead zone') that extends up to the 'light cylinder' at distances

$$r_{lc} \equiv c/\Omega_* = 1.6 \times 10^8 \mathrm{cm} \left(\frac{P_*}{33\mathrm{ms}}\right) \quad (1)$$

from the rotation axis ($\Omega_*$ is the angular velocity and $P_* \equiv 2\pi/\Omega_*$ the period of the rotating neutron star), and two open line regions that originate around the two stellar magnetic poles (the so called 'polar caps'). From each polar cap outflows the main magnetospheric current, which in the case of the aligned rotator may be estimated as

$$I = \mp 1.23 \frac{B_* r_*^3 \Omega_*^2}{4c} \ . \quad (2)$$

Here, $B_* \sim 10^{13}$G and $r_* \sim 10^6$cm are the stellar polar magnetic field and radius respectively (Gruzinov 2004; Contopoulos 2005). The $\mp$ sign in eq. (2) depends on whether the magnetic axis is aligned or counter-aligned with the axis of rotation (our results will heretofore refer to the aligned case with the corresponding result for the counter-aligned case in parentheses). CKF established that the return electric current flows along the separatrix between open and closed field

⋆ E-mail: icontop@academyofathens.gr

lines. In fact, they self-consistently determined the distribution of electric current as well as the distribution of electric space-charge everywhere in the magnetosphere. We would like to point out here that magnetohydrodynamics does not deal with the issue of how this is materialized with actual distributions and flows of charged particles (electrons and positrons). This is not really a problem for the largest part of the magnetosphere since it is known that the number density of the electron-positron plasma that fills the magnetosphere exceeds the above space-charge by a huge multiplicity factor (on the order of $10^3 - 10^4$; e.g. Arons 1983), and all that is needed in order to obtain the distributions required by CKF is a *slight difference in the velocities of electrons and positrons*. As we will now argue, this may not be true in the separatrix between open and closed field lines.

## 2 THE PULSAR SYNCHROTRON

We will discuss here only the axisymmetic case (we plan to address the 3D problem in Paper II of this series based on the numerical results of Kalapotharakos & Contopoulos 2009). Inside the closed line region, $B_\phi = 0$, and particles at its tip corotate with Lorentz factor $\gamma$ equal to

$$\gamma \equiv \frac{1}{\sqrt{1-(R\Omega_*/c)^2}} \approx \frac{1}{\sqrt{2(r_{lc}-R)/r_{lc}}} \ , \tag{3}$$

where, $R \approx r_{lc}$ is the (cylindrical) distance from the rotation axis. Let us heretofore denote quantities at the inner/outer surface of the separatrix with $\mp$ indices respectively. The toroidal magnetic field $B_\phi^- = 0$, and

$$B_\phi^+ = \frac{2I}{cR} \ . \tag{4}$$

Uzdensky (2003) and others pointed out that, as the tip of the dead zone approaches the light cylinder, the poloidal magnetic field $B_p^-$ diverges as

$$\frac{B_p^-}{B_\phi^+} = \gamma \tag{5}$$

and $B_p^+ = 0$ (the Lorenz invariant $B^2 - E^2$ is continuous across the separatrix, and $E = R\Omega_* B_p/c$; see Ffig. 1; see also fig. 4 of Kalapotharakos & Contopoulos 2009, fig. 11 of Timokhin 2006, and fig. 1 of Spitkovsky 2006).

Note that particles at the tip of the dead zone corotate with the star due to the combined action of the magnetospheric electric and magnetic fields. During that motion, they deviate around their corotation radius within distances on the order of the gyroradius

$$\begin{aligned} d &\approx \frac{\gamma m_e c^2}{eB_p^-} = \frac{m_e c^2}{eB_\phi^+} \equiv \frac{c}{\omega_B} \\ &\approx 10^{-3}\mathrm{cm}\left(\frac{B_*}{10^{13}\mathrm{G}}\right)^{-1}\left(\frac{P_*}{33\mathrm{ms}}\right)^3 \ . \end{aligned} \tag{6}$$

Here, $m_e$, $e$ are the electron mass and charge respectively, and $\omega_B \equiv eB_p^-/\gamma m_e c$ is the gyration frequency. For a 'cold' particle distribution, *this distance dictates also the thickness of the separatrix layer*. We will assume that the closed line region extends as close to the light cylinder as is allowed by the equations of motion[1], namely that

$$d \approx r_{lc} - R = \frac{r_{lc}}{2\gamma^2} \ . \tag{7}$$

Eqs. (6) & (7) yield

$$\begin{aligned} \gamma &= \sqrt{\frac{r_{lc}}{2d}} \equiv \sqrt{\frac{\omega_B}{2\Omega_*}} \\ &\approx 3\times 10^5\left(\frac{B_*}{10^{13}\mathrm{G}}\right)^{1/2}\left(\frac{P_*}{33\mathrm{ms}}\right)^{-1} \ . \end{aligned} \tag{8}$$

One interesting feature of the separatrix is that it is negatively (positively) charged with surface charge density

$$\sigma \equiv \frac{E^+ - E^-}{4\pi} \approx \mp\frac{B_p^-}{4\pi} \ . \tag{9}$$

We can express the number density $n$ of charge carriers in the separatrix layer as

$$n \equiv \kappa\frac{\sigma}{ed} = \kappa\frac{(B_p^-)^2}{4\pi\gamma m_e c^2} \ . \tag{10}$$

Obviously, *the multiplicity factor $\kappa$ must be on the order of unity for the force-free assumption to be valid*. Note that at the tip of the dead zone, the Goldreich-Julian number density $n_{GJ}$ is equal to

$$n_{GJ} \equiv \frac{-\mathbf{B}\cdot\mathbf{\Omega}_*}{2\pi ec[1-(R/r_{lc})^2]} \approx \frac{B_p^-}{4\pi ed} = \frac{(B_p^-)^2}{4\pi\gamma m_e c^2} \tag{11}$$

(Goldreich & Julian 1969, CKF), and therefore,

$$\begin{aligned} n &\approx n_{GJ} \\ &= 6\times 10^{22}\mathrm{cm}^{-3}\left(\frac{B_*}{10^{13}\mathrm{G}}\right)^{5/2}\left(\frac{P_*}{33\mathrm{ms}}\right)^{-7} \ . \end{aligned} \tag{12}$$

We have shown here that the number density of charge carriers at the tip of the separatrix must be close to the minimum number density needed to support the surface charge density required by eq. (9). These particles corotate with the star at speeds very close to the speed of light. If we now apply Ampère's law

$$B_p^- = \frac{4\pi}{c}\frac{\mathrm{d}I_\phi}{\mathrm{d}l} \approx 4\pi\sigma c \ , \tag{13}$$

and if we assume that particles at the tip of the separatrix move with velocities $\vec{\beta}c$, then eqs. (13) & (4) imply that

$$\frac{\beta_p}{\beta_\phi} \approx \beta_p \sim \frac{B_\phi^+}{B_p^-} = \frac{1}{\gamma} \ . \tag{14}$$

Note that the separatrix is negatively (positively) charged, and therefore, $\vec{\beta}$ points along the direction of stellar rotation and towards the star. In other words, *electrons (positrons) in the separatrix follow a spiral motion as they move inwards away from the tip of the closed line region, with very small pitch angles on the order of* $1/\gamma$ (fig. 2).

CKF (and for that matter all subsequent investigations) failed to emphasize the significance of this annular (i.e. azimuthal) electric current. These electrons/positrons emit incoherent synchrotron radiation up to a cutoff frequency

$$\nu_c \equiv \frac{3\gamma^3 c}{2\pi r_{lc}} = \frac{3\gamma^3}{P_*}$$

[1] That is, we will ignore here previous solutions (Contopoulos 2005; Timokhin 2006) which suggested that the dead zone may end at any distance inside the light cylinder.

$$\approx \quad 2\times 10^{18}\mathrm{Hz}\left(\frac{B_*}{10^{13}\mathrm{G}}\right)^{3/2}\left(\frac{P_*}{33\mathrm{ms}}\right)^{-4} \quad , \qquad (15)$$

which corresponds to hard X-rays. We emphasize once again that this incoherent synchrotron radiation is due to the macroscopic corotating motion of the separatrix electrons (positrons) around the light cylinder. We would like to name this configuration *'the pulsar synchrotron'*.

## 3 COHERENT RADIO EMISSION

What remains to be calculated is the total power radiated from such an electron (positron) configuration. The power radiated by an individual particle is equal to

$$L_e = \frac{2}{3}\frac{e^2 c}{r_{lc}^2}\gamma^4 \sim 10^{-3}\mathrm{erg\ s^{-1}}\left(\frac{B_*}{10^{13}\mathrm{G}}\right)^2\left(\frac{P_*}{33\mathrm{ms}}\right)^{-6} \quad , \qquad (16)$$

with a frequency distribution (in erg/s/Hz)

$$F_\nu = 3.23\frac{e^2}{cP_*}(\nu P_*)^{1/3} \qquad (17)$$

at low frequencies $\nu \ll \nu_c$ (Jackson 1975). As seen in fig. (2), the annular volume where radiating electrons/positrons attain their maximum Lorentz factor given by eq. (8) has thickness and height comparable to $d$, and contains

$$N_e \sim 2\pi n r_{lc} d^2 \approx 8\times 10^{25}\left(\frac{B_*}{10^{13}\mathrm{G}}\right)^{1/2} \qquad (18)$$

particles. The total incoherent power emitted by these particles is probably too low to be observable. As we will now argue, however, coherency effects may become very important in the radio frequency range around 100 MHz.

It is well known that, in laboratory synchrotrons, particles travel in bunches with macroscopic dimensions (∼mm) along their direction of motion, where the bunch length $\lambda$ is determined by the geometrical and operational characteristics of the synchrotron. It has been observed that, *at wavelengths comparable to the bunch length (or the length of any structure in the bunch), the radiation from multiple particles is in phase*, giving a radiated power proportional to $N^2$ times the power radiated by an individual particle, where $N$ is the bunch population (e.g. Venturin *et al.* 2005). This emission is orders of magnitude stronger than the incoherent power at those wavelengths, which is proportional to $N$. A practical application of this effect is the generation of THz coherent synchrotron radiation in synchrotrons with X-ray incoherent synchrotron radiation (e.g. Sannibale *et al.* 2003). The pulsar synchrotron is certainly very different from an earth synchrotron. Nevertheless, we may also obtain a characteristic bunch length $\lambda$ in the pulsar synchrotron as follows: separatrix electrons/positrons stay in the annular volume of maximum Lorentz factor at the tip of the dead zone for a path-length on the order of

$$\lambda \sim d\gamma \sim \frac{r_{lc}}{2\gamma} \sim 3\times 10^2\mathrm{cm}\left(\frac{B_*}{10^{13}\mathrm{G}}\right)^{-1/2}\left(\frac{P_*}{33\mathrm{ms}}\right)^2 \qquad (19)$$

(fig. 2). If indeed particles emit coherently at the above characteristic wavelength during the time they need to cross the region of maximum Lorentz factor, the coherent radiation corresponds to about 100 MHz. The annular radiating volume consists of

$$\mu = \frac{2\pi r_{lc}}{\lambda} = 4\pi\gamma \sim 3\times 10^6\left(\frac{B_*}{10^{13}\mathrm{G}}\right)^{1/2}\left(\frac{P_*}{33\mathrm{ms}}\right)^{-1} \qquad (20)$$

regions of length $\lambda$, each one consisting of $N \equiv N_e/\mu$ particles. The total luminosity of the coherent emission in a frequency range on the order of $c/\lambda$ may be estimated as the sum of the luminosities of the $\mu$ coherently emitting regions

$$\begin{aligned} L \quad &\sim \quad 2\mu N^2 \nu F_\nu|_{\nu=c/\lambda} \\ &\sim \quad 4\times 10^{28}\mathrm{erg\ s^{-1}}\left(\frac{B_*}{10^{13}\mathrm{G}}\right)^{7/6}\left(\frac{P_*}{33\mathrm{ms}}\right)^{-7/3} \end{aligned} \qquad (21)$$

(the factor of 2 accounts for the contribution to the total radio luminosity from both hemispheres of the dead zone separatrix).

This is just an order of magnitude calculation of the coherent radio luminosity expected from the tip of the dead zone. More detailed analysis will require the 3D numerical self-consistent reconstruction of the electric and magnetic field geometry near the tip of the dead zone together with the calculation of separatrix particle orbits (work in progress). Nevertheless, our estimate of the coherent radiation frequency is not far from the observed peak of pulsar radio emission at a few hundred MHz. Moreover, as we can see in fig. (3), our result in eq. (21) is consistent with estimates of the total pulsar radio luminosity obtained from the ATNF pulsar catalogue[2] (Manchester *et al.* 2005). We therefore believe that our scenario merits serious consideration as an alternative to the radio pulsar phenomenon.

## 4 DISCUSSION

The scenario that pulsar radio emission may be coming from the light cylinder is not new. In the early days of pulsar astronomy, people discussed the possibility that radio pulses may be due to hot plasma corotating at discrete positions on the light cylinder (e.g. Gold 1968, 1969; Bartel 1978; Cordes 1981; Ferguson 1981). These models have since been abandoned. Our present model is different in several respects (our plasma is cold in its rest frame, the fundamental synchrotron radiation frequency is the neutron star rotation frequency, pulses are due to the 3D structure of the magnetosphere, etc.).

We would like to conclude this presentation with two final points of interest. The first has to do with one of the few robust facts about pulsar radio emission, namely the characteristic S-curve polarization sweeps. In order for our model to survive as a valid alternative to highly successful phenomenological models such as the rotating vector model of Radhakrishnan & Cooke (1969), it has to be able to explain this fact. This analysis requires knowledge of the 3D structure of the pulsar magnetosphere obtained

[2] Our estimates are obtained as follows: for each catalogued pulsar with available radio brightness data we calculate the ON brightness as $P_*/W$ times the average brightness, where $W$ is the observed pulse width. The total radio luminosity is then calculated in the context of the pulsar synchrotron model in which radiation is emitted within $\pm 1/\gamma$ radians above and below the equator. This is very different from the canonical model where radio emission is produced in two beams originating in the polar caps.

only recently by Spitkovsky (2006) and Kalapotharakos & Contopoulos (2009). Let us, however, present here some preliminary results, and let us introduce the three basic angles of the 3D problem, namely the angle $\alpha$ between the rotation axis and the stellar magnetic moment, the angle $i$ between the observer line of sight and the rotation axis, and the observed polarization angle $\psi$ with $\psi = 0$ along the rotation equatorial plane. Let us also introduce the angle $\xi$ between the rotation equatorial plane and the direction connecting the central star with the instantaneous position of the tip of the dead zone on the light cylinder. In the context of our present pulsar synchrotron model, radiation is observed whenever the instantaneous direction of the annular current at the tip of the dead zone happens to lie close to our line of sight. The instantaneous direction of polarization $\psi$ lies along the direction of the instantaneous radius of curvature which, we argue, must be close to $\xi$. Therefore, $\psi \sim \tan^{-1}[\tan(\xi)\sin(i)]$. In fig. (4) we show the variation of $\xi$ with pulsar longitude as obtained in the solution of Kalapotharakos & Contopoulos (2009) for inclination $\alpha = 60^o$. We also plot the resulting polarization sweep for an observer inclination $i = 30^o$. This preliminary result is promising enough to justify the continuation of our effort in paper II of this series.

The second point of interest has to do with the equatorial return current sheet beyond the light cylinder. One can directly check that this is positively (negatively) charged, that is with a surface charge *opposite* to that of the separatrix current sheet inside the light cylinder. And yet, the electric current in both current sheets flows in the same direction, that is towards (away from) the star. Given the limitation on the available number density of charge carriers imposed by the force-free approximation (see discussion in § 2), in order to supply the inward flowing electrons (positrons) and the outward flowing positrons (electrons), we need a source of pairs at the tip of the separatrix at the position of the light cylinder. This may either be supplied as a steady stream of pairs along the separatrix from the surface of the star, or through pair creation by some yet to be determined process at that position. Note that as these particles move away from the tip of the dead zone, they either move along the equator in a trajectory which becomes asymptotically radial (i.e. with a radius of curvature much larger than $r_{lc}$), or they move inwards where the corotation Lorentz factor becomes smaller and smaller. In both cases, their contribution to the total synchrotron radiation energy content is expected to be much smaller than the radiation they emit as they traverse the annular volume of thickness $d$ just inside the light cylinder that we discussed in the previous section.

## ACKNOWLEDGMENTS

We would like to thank G. Contopoulos, C. Efthymiopoulos, C. Kalapotharakos and D. Kazanas for stimulating discussions, and the referee, A. Spitkovsky, for his constructive criticism.

## REFERENCES

Arons, J. 1983, in 'Electron-Positron Pairs in Astrophysics', eds. M. L. Burns, A. K. Harding & R. Ramaty, 163 (New York: American Institute of Physics)
Bartel, N. 1978, A& A, 62, 393
Contopoulos, I., Kazanas, D. & Fendt, C. 1999, ApJ, 511, 351 (CKF)
Contopoulos, I. 2005, A& A, 442, 579
Cordes, J. M. 1981, in 'Pulsars: 13 years of research on neutron stars', Proc. of the Symposium, 115 (Bonn: Dordrecht)
Ferguson, D. C. 1981, in 'Pulsars: 13 years of research on neutron stars', Proc. of the Symposium, 141 (Bonn: Dordrecht)
Gold, T. 1968, Nature, 218, 731
Gold, T. 1969, Nature, 221, 25
Goldreich, P. & Julian, W. H. 1969, ApJ, 157, 869
Gruzinov, A. 2005, Phys. Rev. Lett., 94, 021101
Jackson, W. D. 1975, Classical Electrodynamics (New York: Wiley)
Kramer, M., Wex, N., & Wielebinski, R. 2000, in Pulsar Astronomy - 2000 and beyond, ASP Conf. Series, 202
Kramer, M., Xilouris, K. M., Jessner, A., Lorimer, D. R., Wielebinski, R., & Lyne, A. G. 1997, A& A, 322, 846
Manchester, R. N., Hobbs, G. B., Teoh, A. & Hobbs, M. 2005, AJ, 129, 1993
Kalapotharakos, C. & Contopoulos, I. 2009, A& A, in press
Radhakrishnan, V. & Cooke, D. J. 1969, AL, 3, 225
Sannibale, F., Byrd, J. M. Loftsdottir, A., Martin, M. C., & Venturini, M. 2003, in Proc. of the 2003 Particle Accelerator Conference, IEEE
Spitkovsky, A. 2006, ApJ, 648, L51
Timokhin, A. N., 2006, MNRAS, 368, 1055
Uzdensky, A. D. 2003, ApJ, 598, 446
Venturini, M.,Warnock, R., Ruth, R., & Ellison, J. A. 2005, PhysRevSTAB, 8, 014202

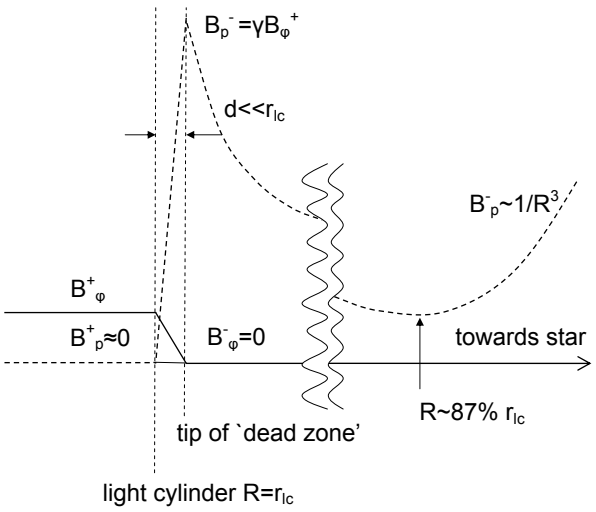


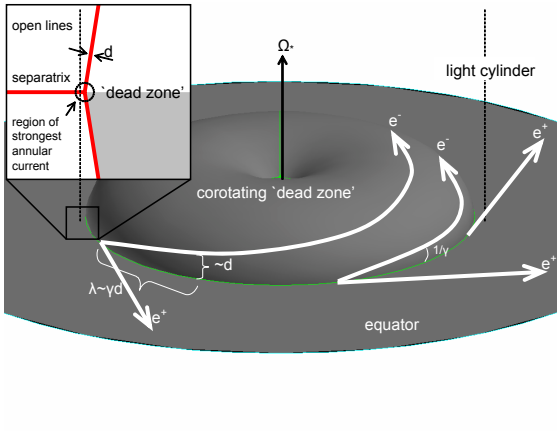


**Figure 1.** Schematic of the dependence of the poloidal (dashed line) and toroidal (solid line) magnetic field components on radial distance $R$ from the star along the equator near the tip of the dead zone. The poloidal field varies as $\propto 1/R^3$ near the star, reaches a minimum value at 87% of the light cylinder distance, grows to a very large value at the tip of the dead zone as given by eq. 5, and drops to zero outside. The toroidal field is zero inside the dead zone, and rises to some finite value outside. The jumps in $B_p$ and $B_\phi$ at the tip of the dead zone take place over some finite distance $d \ll r_{lc}$.

**Figure 2.** Schematic of electron and positron trajectories along the separatrix and the equatorial current sheet respectively for aligned magnetic and rotation axes, and detail of the tip of the dead zone. The light cylinder is denoted with a dashed line. $d \sim 10^{-3}$ cm is the separatrix thickness. $\lambda \sim 1$ m is the electron path length in the pulsar synchrotron.

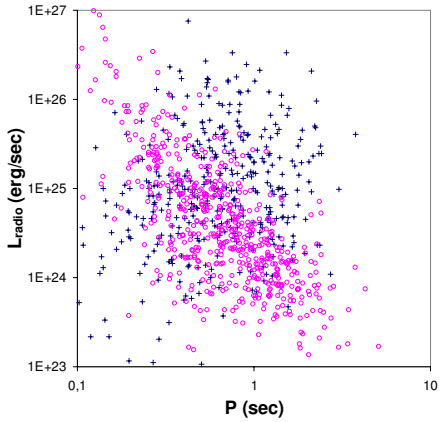


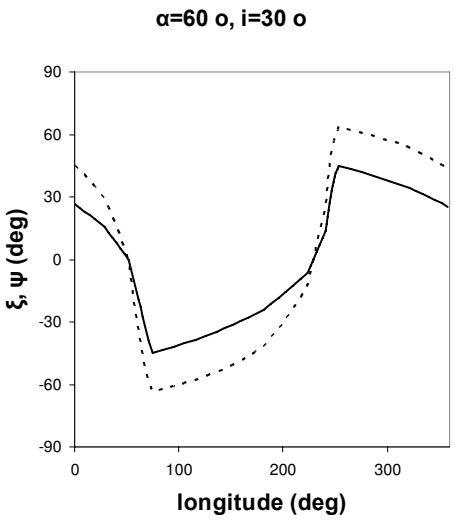


**Figure 3.** Pulsar radio luminosity as a function of the pulsar period. Open circles: calculated according to eq. 21. Crosses: estimated from the observed emission at 400 MHz adjusted in the context of the pulsar synchrotron model where radiation is emitted within $\pm 1/\gamma$ radians above and below the equator instead of in two beams originating in the polar caps. Data are taken from the ATNF pulsar catalogue.

**Figure 4.** Distribution of $\xi$ (dotted line) and estimate of polarization angle $\psi$ (solid line) as functions of the pulsar longitude obtained from the numerical solution of Kalapotharakos & Contopoulos (2009) for $\alpha = 60^o$ and $i = 30^o$.